11th World Congress on Computational Mechanics (WCCM XI)
5th European Conference on Computational Mechanics (ECCM V)
6th European Conference on Computational Fluid Dynamics (ECFD VI)
E. Oñate, J. Oliver and A. Huerta (Eds)

VOLUME CONSERVATION OF 3D SURFACE TRIANGULAR MESH SMOOTHING

DANIEL RYPL* AND JIŘÍ NERAD†

* Czech Technical University in Prague
Faculty of Civil Engineering, Department of Mechanics
Thákurova 7, 166 29 Prague, Czech Republic
e-mail: daniel.rypl@fsv.cvut.cz

†Czech Technical University in Prague
Faculty of Civil Engineering, Department of Mechanics
Thákurova 7, 166 29 Prague, Czech Republic
e-mail: jiri.nerad@fsv.cvut.cz

Key words: 3D Surface, Mesh Optimization, Laplacian Smoothing, Volume Conservation, Closed and Open Surfaces

Abstract. Present paper deals with a shrinkage free smoothing of triangular isotropic meshes over three-dimensional surfaces. Adopted approach is based on Laplacian smoothing combining in alternating manner positive and negative weights in consecutive cycles of the smoothing. Since the aim is to improve the shape of individual elements of the mesh rather than to get rid of noise, the weights are derived in a very simple way using a "do-not-harm" concept. The paper also extends the application of the smoothing from closed surfaces to open surfaces and their combination. The performance and capabilities of the presented methodology are demonstrated on several examples.

1 INTRODUCTION

Laplacian smoothing is a commonly used technique to improve quality of (not only) finite element meshes. Its popularity resides in simple and efficient implementation and good performance (especially) on isotropic simplicial meshes. While its application to 3D and planar 2D meshes is straightforward, use for 2.5D meshes on curved surfaces suffers from (usually undesirable) shrinkage as the smoothed node is attracted toward center of curvature. This can be efficiently prevented by returning the smoothed nodes back onto the surface. This is quite easy if analytical (typically parametric) description of the underlying surface is available. But this may be not always the case, for example when handling discretely described surfaces.

In past, different approaches for reducing the noise of a surface mesh while preventing its shrinkage were developed. Some algorithms [1, 2, 3] are based on the local volume control using vertex balance procedure. Other techniques [4, 5] combine the shrinkage phase with an expansion phase during each smoothing cycle. While the approach in [4], implemented as a low pass filter removing high curvature variations, is utilising two smoothing subcycles (within each smoothing cycle), one with positive weights, the other one with negative weights, authors of [5] combine (within each smoothing cycle) smoothing of points with smoothing applied to differences between points before and after their smoothing. In [6], a shrinkage-free interpolatory smoothing, based on the assumption that centers of all (arbitrarily polygonal) facets of the mesh are located on the anticipated geometry of the surface, is introduced. The smoothing scheme is applied to a larger stencil of previously subdivided mesh using the $\sqrt{3}$ splitting. A small shrinkage induced due to the linear approximation is then eliminated by the application of the Taubin-like inflation operator. In other works [7, 8], the Laplacian diffusion equation was replaced by mean curvature flow, allowing surface nodes to move only along the surface normal. This concept was later extended also to Gaussian curvature flow [9].

In this work, a similar approach to that presented in [4] is employed. However, the weights for shrinkage and expansion smoothing subcycles are derived (contrary to [4], where they are determined by spectral analysis using the Fourier transform) using the "do-not-harm" concept, the idea of which is to bring a node on the optimal mesh back to its original position after both subcycles. The expansion weight is dependent on the shrinkage weight and is computed directly from the geometrical setting just before the shrinkage subcycle is started. Note that the algorithm was derived for in-plane smoothing of surface meshes without analytical description of the underlying surface. This implies that it is assumed that the nodes of the original mesh are located on the surface. The application of the algorithm to meshes with random noise in the sense of out-of-surface deviation is under investigation.

The paper is organized as follows. In Section 2, the determination of smoothing weights is outlined. The application of the volume preserving smoothing to open surfaces is elaborated in Section 3. Several examples demonstrating the performance of the proposed methodology are presented in Section 4. Section 5 then summarizes the paper with concluding remarks.

2 ASSESSMENT OF SMOOTHING WEIGHTS

The smoothing weights are derived using the "do-not-harm" concept, the idea of which is to bring a node on the optimal mesh back to its original position. Let's consider two consecutive smoothing cycles of a regular polygon over a circle of radius r (see Figure 1). In both cycles, each node is repositioned to a new location given by a weighted average of the node itself and its neighbours. Particularly, during the first smoothing cycle, node P,

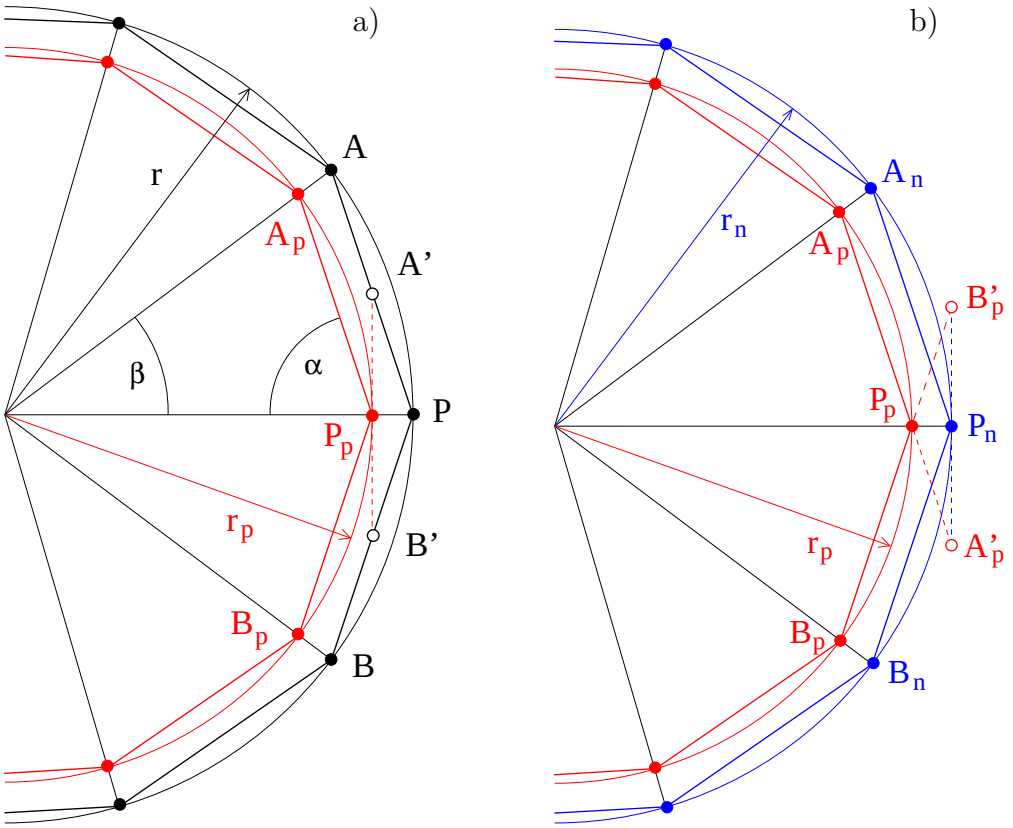

Figure 1: Two subcycles of smoothing: (a) shrinkage (using positive weight λ), (b) expansion (using negative weight μ).

given by a positional vector $\boldsymbol{P}$, is shifted to the new position $\boldsymbol{P}_p$ (Figure 1a) given by

$$\begin{aligned} \boldsymbol{P}_p &= \frac{1}{2}(\boldsymbol{A}' + \boldsymbol{B}') = \\ &= \frac{1}{2}\Big(\big((1-\lambda)\boldsymbol{P} + \lambda\boldsymbol{A}\big) + \big((1-\lambda)\boldsymbol{P} + \lambda\boldsymbol{B}\big)\Big) = \\ &= (1-\lambda)\boldsymbol{P} + \lambda\frac{1}{2}(\boldsymbol{A} + \boldsymbol{B}) \ , \end{aligned} \tag{1}$$

where λ is a positive weight (therefore subscript p is used for repositioned nodes). Because of the regularity of the initial polygon and because the same λ is used for each node, all the repositioned nodes are located again on a circle (centered at the same point as the original circle), this time, however, of radius r_p. Since $\lambda > 0$, $r_p < r$ and shrinkage of the initial polygon is observed. To enforce its expansion, the second smoothing cycle, during

which node P_p is moved from location $\boldsymbol{P}_p$ to position $\boldsymbol{P}_n$ (Figure 1b) given by

$$\begin{aligned} \boldsymbol{P}_n &= \frac{1}{2}(\boldsymbol{A}'_p + \boldsymbol{B}'_p) = \\ &= \frac{1}{2}\Big(\big((1-\mu)\boldsymbol{P}_p + \mu\boldsymbol{A}_p\big) + \big((1-\mu)\boldsymbol{P}_p + \mu\boldsymbol{B}_p\big)\Big) = \\ &= (1-\mu)\boldsymbol{P}_p + \mu\,\frac{1}{2}(\boldsymbol{A}_p + \boldsymbol{B}_p)\ , \end{aligned} \tag{2}$$

is performed with a negative (subscript n) weight μ. After the second smoothing cycle, all the nodes will be regularly spaced on a co-centered circle with radius r_n. The goal is to ensure that $r = r_n$. The shrinkage and expansion of the radius of the underlying circle during the first and second smoothing cycle, respectively, can be represented as

$$r - r_p = \lambda(r - r\cos\beta)\ , \tag{3}$$

$$r_p - r_n = \mu(r_p - r_p\cos\beta)\ . \tag{4}$$

By summing Eqs (3) and (4) and setting $r = r_n$, one will obtain

$$0 = (\lambda r + \mu r_p)(1 - \cos\beta)\ , \tag{5}$$

that can be simplified (as $\beta > 0$ and thus $1 - \cos\beta \neq 0$) to

$$\frac{r}{r_p} = -\frac{\mu}{\lambda}\ , \tag{6}$$

which verifies $|\mu| > \lambda > 0$ [4]. Expressing r_p from Eq. (3) and substituting it to Eq. (6) yields

$$\frac{1}{1 - \lambda(1 - \cos\beta)} = -\frac{\mu}{\lambda}\ . \tag{7}$$

Finally, by considering $1 - \cos\beta = 2\cos^2\alpha$, the final relationship for μ reads

$$\mu = \frac{\lambda}{2\lambda\cos^2\alpha - 1}\ . \tag{8}$$

For irregular polygon, $\cos^2\alpha$ in Eq. (8) is replaced by (optionally weighted) average of square of cosines of angles between the normal at node P and segments of the polygon incident at node P. Normal at P is approximated by a simple average of normals to both edges sharing node P in plane given by these edges. If the edges are parallel, $\cos^2\alpha$ is equal to zero.

Similarly, when smoothing a node on a surface (see Figure 2), $\cos^2\alpha$ is calculated as (optionally weighted) average of square of cosines of angles α_j between the normal $\boldsymbol{n}_P$ at node P and edges connecting node P with surrounding nodes Q_j. Normal $\boldsymbol{n}_P$ is evaluated

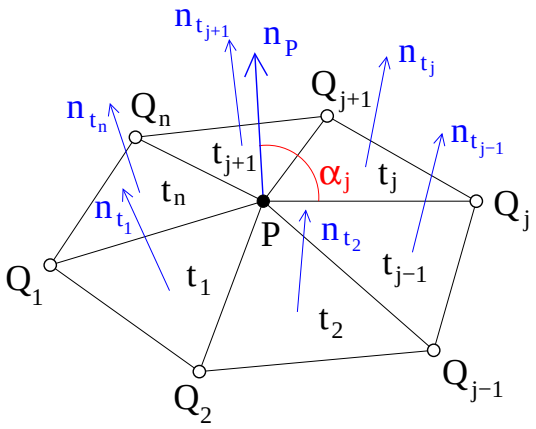

Figure 2: Geometrical setup for the evaluation of smoothing weights for inner node P on a surface.

as weighted average of normals $\boldsymbol{n}_{t_j}$ of triangular elements t_j sharing node P (see Figure 2) with weights proportional to their area.

Note that when smoothing mesh on a straight curve or planar surface (for which $\cos^2\alpha = 0$), Eq. (8) yields $\mu = -\lambda$, which is known as bi-Laplacian smoothing.

Now, assuming that the initial position of node P (before smoothing is invoked) is denoted as $\boldsymbol{P}^1$, the position of node P on a closed smooth (C^1 continuous) surface or curve after $i = 1, 2, \ldots$ smoothing cycles (total number of which is even) is given by

$$\boldsymbol{P}^{i+1} = (1 - w)\boldsymbol{P}^i + \frac{w}{n}\sum_{j=1}^{n} \boldsymbol{Q}_j^i \ , \tag{9}$$

where weight w is equal to λ in the odd smoothing cycle and to μ in the even smoothing cycle, and n is the number of nodes Q_j connected to node P by an edge. Note that weight μ used in the even smoothing cycle is calculated from the geometrical setting just before the preceding odd smoothing cycle is started.

3 SMOOTHING OF OPEN SURFACES

If the surface to be processed is not closed or smooth, a special treatment is necessary to preserve sharp features. In the present work, all sharp features (as boundary curves of an open surface) are assumed to be topologically explicitly present in the geometry description. This enables to perform the smoothing hierarchically, from vertices (which are kept intact), over curves to surfaces, while always applying the smoothing only to inner nodes of processed entity. However, proper application of expansion phase to nodes adjacent to boundary requires appropriate representation of shrinkage phase at adjacent boundary nodes.

In order to determine the shrinkage at vertex V at a free end of an open curve (see Figure 3), the curve is extended by a fictitious segment e' mirroring the utmost edge e of

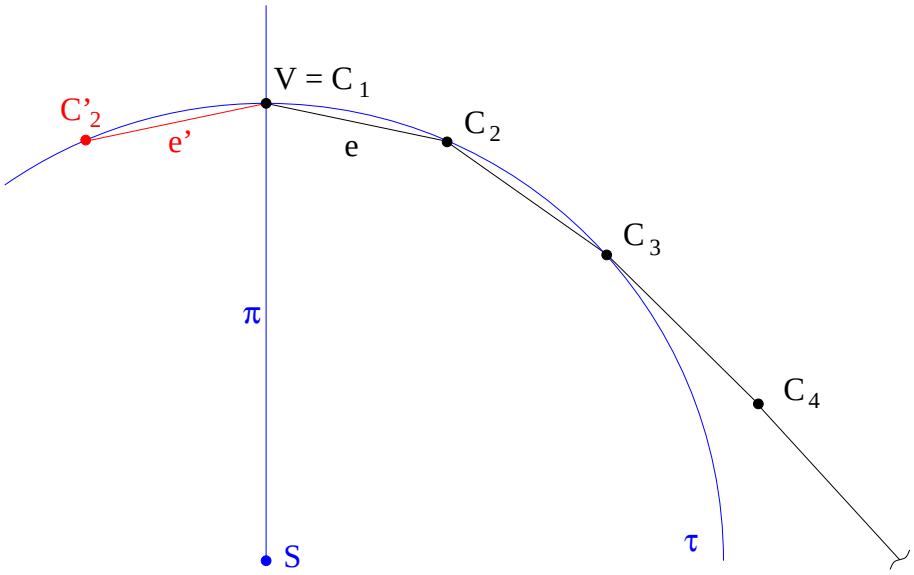

Figure 3: Geometrical setup for the assessment of shrinkage at vertex V of an open curve.

the curve with respect to a plane π normal to the curve and passing through the vertex V. This makes the vertex (temporarily) an inner node, for which the shrinkage in the odd smoothing cycle can be computed according to Eq. (9). During expansion phase (even cycle of the smoothing), the vertex is returned to its original position. Since only discrete representation of the curve is available, the mirroring plane π is approximated by a plane which is perpendicular to the plane τ given by utmost three nodes on the curve ($V = C_1$, C_2 and C_3) and which is passing through vertex V and center S of a circle passing through those nodes. If the nodes are co-linear, the mirroring plane is perpendicular to the utmost edge e.

When assessing the shrinkage at nodes on a curve bounding an open surface, the above concept of mirroring is somewhat cumbersome and therefore a different approach, mimicking the behaviour of nodes in the neighbourhood, is adopted. In this approach, the shrinkage s at a particular curve node P is calculated as an average of normal components of shifts (during the odd smoothing cycle) of m neighbour inner surface nodes Q_j (see Figure 4)

$$s = \frac{1}{m}\sum_{j=1}^{m} s_j = \frac{1}{m}\sum_{j=1}^{m}(\boldsymbol{Q}_j^{i+1} - \boldsymbol{Q}_j^{i}) \cdot \boldsymbol{n}_{Q_j} \ . \tag{10}$$

Shifted position of curve node P is then evaluated simply as

$$\boldsymbol{P}^{i+1} = \boldsymbol{P}^{i} + s\boldsymbol{n}_P \ . \tag{11}$$

During expansion in the even smoothing cycle, the curve node is moved back to its original position. The same concept is used for the evaluation of shrinkage at vertex of a curve bounding the surface.

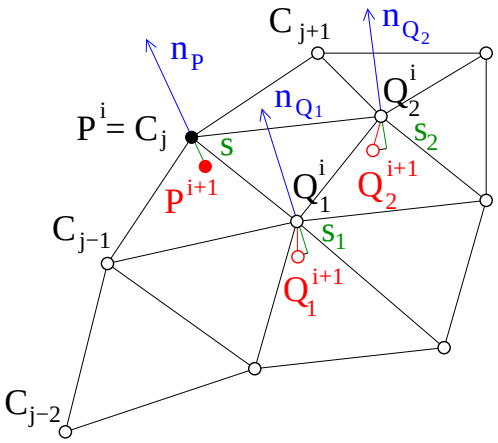

Figure 4: Geometrical setup for the assessment of shrinkage at curve node P of an open surface.

4 NUMERICAL EXAMPLES

The performance of the proposed volume preserving smoothing is demonstrated on two examples. In the first one, smoothing of a closed mesh over a sphere of unit radius is presented. The surface of the sphere was initially discretized by a uniform (nearby optimal) mesh, which was then randomly perturbed on one half of the sphere. The mesh was optimized using altogether 40 cycles (20 cycles, each with two subcycles) of smoothing with λ set to 0.5. The example was run for three different mesh densities. The results in terms of the change of volume, deviation of nodes from the exact surface and mesh quality are summarized in Table 1. Quality of individual elements is assessed using the ratio of radii of inscribed and circumscribed circle normalized to interval $\langle 0; 1\rangle$ (with 1 being the quality of equilateral triangle). The results reveal a negligible shrinkage, far below 1 % in all cases, which is quickly decreasing with the growing mesh density. The quality of the

Table 1: Summary of qualitative results of smoothing of surface meshes over a unit sphere (Elements - number of elements, ΔV - relative change of volume (shrinkage < 0), δ_{in} - maximal relative inward deviation from the exact surface, δ_{out} - maximal relative outward deviation from the exact surface, old q_{min} - minimal element quality on the original mesh, new q_{min} - minimal element quality on the smoothed mesh, old $\bar{q}$ - harmonic mean of element quality on the original mesh, new $\bar{q}$ - harmonic mean of element quality on the smoothed mesh).

Elements	ΔV [%]	δ_{in} [%]	δ_{out} [%]	old q_{min}	new q_{min}	old $\bar{q}$	new $\bar{q}$
208	-0.260	3.24	4.13	0.14	0.81	0.86	0.98
816	-0.070	1.10	0.82	0.14	0.82	0.87	0.97
3200	-0.019	0.23	0.19	0.18	0.64	0.88	0.98

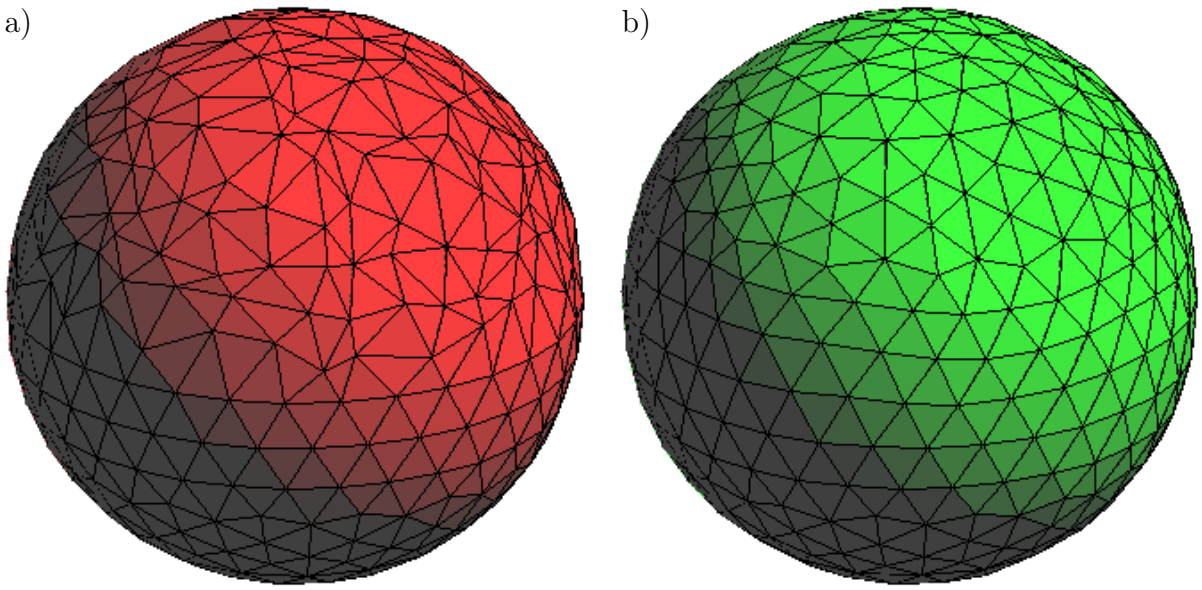

Figure 5: Smoothing of a surface mesh (with 816 elements) over a unit sphere: (a) original mesh (perturbed on the top hemisphere), (b) smoothed mesh.

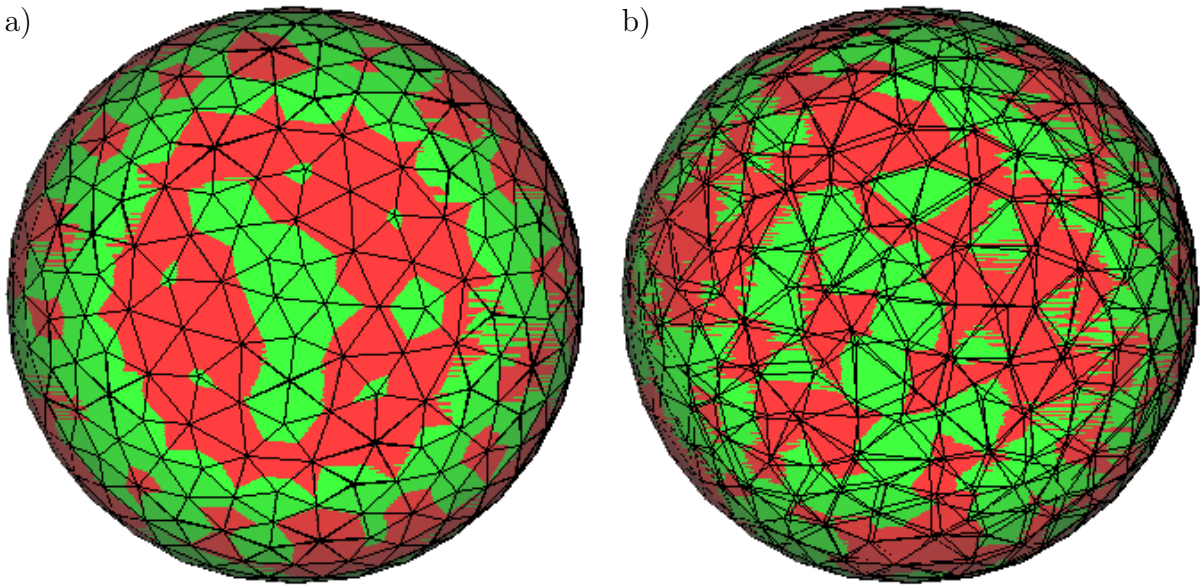

Figure 6: Overlay of original and smoothed mesh (with 816 elements) on a unit sphere: (a) over unperturbed hemisphere, (b) over perturbed hemisphere.

smoothed meshes is improved considerably in all cases. This is demonstrated in Figure 5 that depicts the original and the smoothed mesh of intermediate density (816 elements). In Figure 6, the overlay of the original and smoothed meshes on both hemispheres is displayed.

The second example is a pawn-like figure (see Figure 7) with various principal curvatures, differing also in sign. The side face of the figure is formed by a hyperboloid-like surface, horizontal cut of which is always an ellipse. The bottom and top cuts (treated as sharp features) are geometrically similar ellipses with half-axes in the ratio 2:1. The bottom ellipse is, however, twice as large as the top ellipse and it is rotated with respect to the top ellipse by 90 degs. While the bottom base is flat, there is a half-ellipsoid with half-axes in the ratio 1:2:1 on the top. The surface meshes (again three with different mesh densities) were created in the similar manner as in the first example but this time the whole surface mesh was perturbed. The meshes were again smoothed using 40 cycles of smoothing and using λ equal to 0.5. The results, documenting the relative change of the volume and the quality of the original and smoothed mesh are summarized in Table 2. Although this time the observed relative shrinkage is somewhat larger than in the first example, it is still under control and with the increasing density of the mesh it is steadily decreasing. The images of the original and smoothed mesh (again that of intermediate density - 1426 elements) are shown in Figure 7.

5 CONCLUSIONS

In this paper, a volume preserving smoothing of triangular isotropic meshes over three-dimensional surfaces was presented. The proposed approach is based on Laplacian smoothing switching between positive weights in the odd smoothing cycles, causing a shrinkage, and appropriate negative weights in the even smoothing cycles, eliminating the preceding shrinkage by an expansion. Since the approach is aimed at in-plane smoothing, it is assumed that there is no noise in terms of out-of-surface deviation. This allows to derive a formula for the negative weight using the "do-not-harm" concept that ensures that a node on the optimal mesh is brought back to its original position after the completion of consecutive shrinkage and expansion smoothing cycles. Although the

Table 2: Summary of qualitative results of smoothing of surface meshes over pawn-like figure (the parameters used are the same as in Table 1, except for δ_{in} and δ_{out} which are not available).

Elements	ΔV [%]	old q_{min}	new q_{min}	old $\bar{q}$	new $\bar{q}$
564	-1.071	0.22	0.81	0.79	0.96
1426	-0.140	0.10	0.76	0.79	0.97
5720	-0.035	0.07	0.66	0.78	0.98

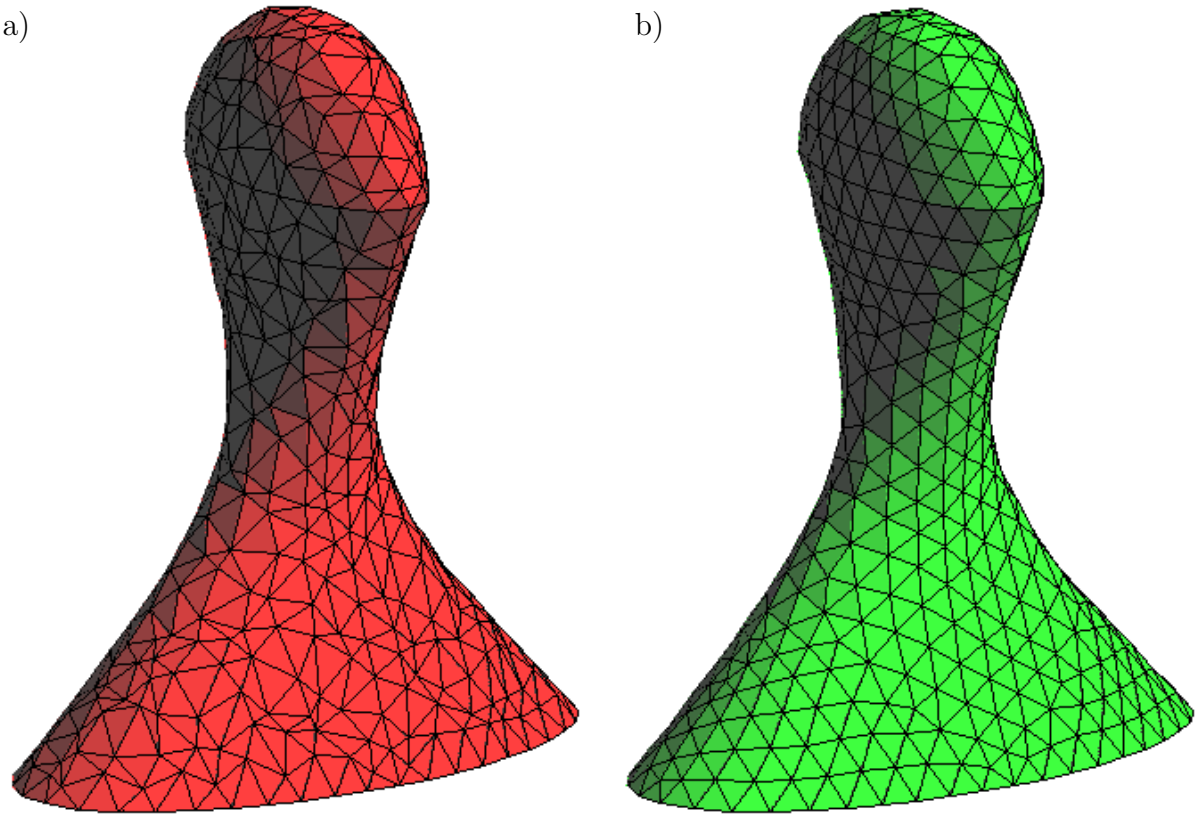

Figure 7: Smoothing of a surface mesh (with 1426 elements) over a pawn-like figure: (a) original mesh, (b) smoothed mesh.

formula is derived for a curve of constant curvature, numerical experiments reveal that it can be successfully applied also to general surfaces. The paper also extends the proposed methodology for smoothing of closed surfaces to open surfaces, for which a special procedure assessing the shrinkage of boundary nodes must be adopted. The capabilities of the presented smoothing approach are demonstrated on two examples which prove that volume conservation is under control also for relatively coarse meshes.

ACKNOWLEDGMENTS

This work was supported by the Technology Agency of the Czech Republic under project No. TA02011196. Its financial assistance is gratefully acknowledged.

REFERENCES

[1] Kuprat, A., Khamayseh, A., George D. and Larkey, L. Volume conserving smoothing for piecewise linear curves, surfaces, and triple lines. *Journal of Computational*

Physics (2001) **172**(1):99–118.

[2] Liu, X.G., Bao, H.J., Shum, H.Y. and Peng, Q. A novel volume constrained smoothing method for meshes. *Graphical Models* (2002) **64**(3–4):169–182.

[3] Sousa, F.F., Castelo, A., Nonato, L.G., Mangiavacchi, N. and Cuminato, J.A. Local volume-conserving free surface smoothing. *Communications in Numerical Methods in Engineering* (2007) **23**:109–120.

[4] Taubin, S. Curve and surface smoothing without shrinkage. *Proceedings of Fifth International Conference on Computer Vision* (1995) 852–857.

[5] Vollmer, J., Menel, R. and Müller, H. Improved Laplacian smoothing of noisy surface meshes. *Computer Graphics Forum* (1999) **18**(3):131–138.

[6] Li, G., Bao, H. and Ma, W. A unified approach for fairing arbitrary polygonal meshes. Graphical Models (2004) **66**(3):160–179.

[7] Desbrun, M., Meyer, M., Schroder, P. and Barr, A.H. Implicit fairing of irregular meshes using diffusion and curvature flow. *ACM SIGGRAPH* (1999) 317–324.

[8] Xu, G. Surface fairing and featuring by mean curvature motions. *Journal of Computational and Applied Mathematics* (2004) **163**:295–309.

[9] Zhao, H. and Xu, G. Triangular surface mesh fairing via Gaussian curvature flow. *Journal of Computational and Applied Mathematics* (2006) **195**(1–2):300-311.

[10] Chen, C.-Y. and Cheng, K.-Y. A sharpness dependent filter for mesh smoothing. *Computer Aided Geometric Design* (2005) **22**:376–391.